Journal of Solid State Chemistry 183 (2010) 595–599

Contents lists available at ScienceDirect

Journal of Solid State Chemistry

journal homepage: www.elsevier.com/locate/jssc

A facile processing way of silica needle arrays with tunable orientation by tube arrays fabrication and etching method

Mingwei Zhu, Haigen Gao, Hongwei Li, Jiao Xu, Yanfeng Chen *

National Laboratory of Solid State Microstructures and Department of Materials Science and Engineering, Nanjing University, Nanjing 210093, People's Republic of China

ARTICLE INFO

Article history:
Received 30 August 2009
Received in revised form
20 December 2009
Accepted 1 January 2010
Available online 11 January 2010

Keywords:
Needle arrays
Tube etching
Silica fiber
Tube arrays

ABSTRACT

A simple method to fabricate silica micro/nano-needle arrays (SNAs) is presented based on tube-etching mechanism. Using silica fibers as templates, highly aligned and free-standing needle arrays are created over large area by simple processes of polymer infiltration, cutting, chemical etching and polymer removal. Their sizes and orientations can be arbitrarily and precisely tuned by simply selecting fiber sizes and the cutting directions, respectively. This technique enables the needle arrays with special morphology to be fabricated in a greatly facile way, thereby offers them the potentials in various applications, such as optic, energy harvesting, sensors, etc. As a demonstration, the super hydrophobic property of PDMS treated SNAs is examined.

1. Introduction

Nano- and micro-needle arrays have received a lot of attention in the recent years. Compared with the rod, wire or tube arrays, the needle arrays have a lower symmetry and special configuration with gradually decreased tips and V-shape interspaces. Such a unique morphology, combined with its dimension and building materials, enable them to have many unique and interesting properties. For example, nano-needle arrays of ZnO, AlN, and graphite show efficient field emission properties [1–4]; silicon nano-needle arrays exhibit much better broad band antireflection property than any other morphology [5–8], etc. Hence, they find applications in areas of optic [5], data recording [9,10], or even transdermal drug delivery [11].

Up to now, only a few materials and methods can be employed to fabricate needle arrays. However, they almost suffer from high cost processing. For example, submicron and micron needle arrays of semiconductors, such as Si and Fe/GaAs, were created by microfabrication techniques of focused ion beam (FIB) [9], reactive ion etching (RIE) [7,12], laser irradiation [6], electron cyclotron resonance (ECR) plasma process [5,13], chemical vapor deposition (CVD) [14], or their combination. Recently, solution reaction based methods attracted much attention. They are simple, efficient and involve no complicated processes or equipments. In these methods, needles are created in solution by either *growth* or *etching*, two contrary processes of "adding" and "taking". ZnO nanoneedles were often grown in solution [15], but silica needle arrays (SNAs) were firstly etched in solution by Brian D'Urso et al. using composition patterned glass rod [16]. More recently, this method was employed by Ming Su et al. to fabricate cone arrays for solar energy conversion [17] or as templates for fabricating other microstructures [18]. During the fabrication of silica needles by chemical etching, the etch-rate contrast played a key role in the formation of needle shape. Instead of the etch-rate contrast realized by the complicated covering another kind of glass on the original fiber [16], here we developed a simple and effective method of tube arrays fabrication and etching (TAFE) for fabricating silica needle arrays (SNAs). Our work was inspired by the tube etching phenomena widely used for fabrication of a single SNOM tip [19,20], during which the etching was confined in a tube formed by the outer organic coating on the optical fiber. Here we created tube arrays and let the silica fibers to be etched in designed confined spaces to realize etch-rate contrast. We show that SNAs with sharp tips could be easily created over large area with tunable geometry and size. We also show that their orientations, which may endow them with some anisotropic properties, could be definitely controlled by this method. As a demonstration for potential application, their hydrophobic property was investigated after being covered with PDMS layers.

2. Experimental

2.1. Outline of the experiment

The SNAs were fabricated through a tube arrays fabrication and etching (TAFE) method. As a preparatory work, the commer-

* Corresponding author.
E-mail address: yfchen@nju.edu.cn (Y. Chen).

0022-4596/$ - see front matter © 2010 Elsevier Inc. All rights reserved.
doi:10.1016/j.jssc.2010.01.001

cially available silica fibers were bound tightly using thread to make them touched etch other and form fiber arrays. Fig. 1 shows the experimental outlines. Firstly, the apertures of the fibers were filled with polymer through a polymer infiltration process (step 1), and then the polymer filled fiber arrays were cut into slices (step 2). In the next step, the slices were etched in an anisotropic way to form the needle shapes (step 3). Finally, the needle arrays were acquired by removal of the filled polymer (step 4). Here we choose polymethyl methacrylate (PMMA) or hydrogenated rosin (HR) as the infiltration polymer to demonstrate the detailed fabrication processes.

2.2. Polymer filling and cutting

Polymers of PMMA or HR were selected to infiltrate fiber arrays according to the fiber diameters. For fibers below tens of micrometers, PMMA was selected for its extremely low viscosity of monomer methl methacrylate (MMA) before polymerization, which enabled it to enter nanosized apertures to realize full filling. For fibers above tens of micrometers, HR was used for its simplicity by just heating up to its melting point in vacuum to facilitate the infiltration. Both PMMA and HR are rigid at temperatures below their glass transition temperatures; also, they are non-water soluble and HF acid resistant. These properties make them form excellent frameworks without deformation during the processes of cutting and etching.

Experimentally, for PMMA infiltration, a bulk polymerization process was firstly carried out. Thirty milligram of benzoyl peroxide (BPO) was dissolved in 30.0 ml of MMA that is purified by rotation evaporator. When the BPO was fully dissolved, the silica fiber arrays were immersed into the solution and followed with ultrasonic wave treatment to make a full infiltration. Then they were placed in a water bath operating at 85 °C until the contents were as viscous as glycerol, which is called prepolymerization. After that they were transferred to another water bath of 40 °C for full polymerization until the contents became a hard solid. For HR infiltration, fiber arrays were placed in HR at room temperature, and then they were vacuumized in vacuum drying chamber and heated up to 150 °C for about 30 min. Finally, they were taken out and cooled down to form a rigid solid composite. The polymer filled fiber arrays are then cut into slices by slicing machine for etching.

2.3. Etching and polymer removal

Etching was carried out in a transparent polymer vessel with a cover to stop the evaporation of HF vapor. The samples were immersed in HF solution with various concentrations at temperature of 30 °C. After etching, they were rinsed with distilled water for five times to remove the remanent HF and then dried in an oven at 50 °C for about 1 h. The infiltrated polymers were removed by sintering at 400 °C for 30 min, or dissolved in trichloromethane for 5 h.

2.4. Characterization

Morphology characterization was conducted using a scanning electron microscope (XL30, Philips) with primary electron energy of 20 kV; a layer of gold was sputtered (Model 682, Gatan) onto samples to facilitate the imaging. Contact angles were measured by a DropMeter A-200 contact angle system (MAIST Vision Inspection & Measurement Ltd Co., China). A drop of distilled water 5 μL in volume was dispensed from a flat-tipped stainless steel needle onto each surface.

3. Results and discussion

Typical SNAs fabricated by the tube-array-etching (TAFE) method are shown in Fig. 2 of scanning electron microscopy (SEM) images. It is seen that all of the needles are of highly uniform tapered shape over large area, and each needle has a smooth surface and sharp tip. These results indicate the effectiveness and efficiency of the present method in mass fabrication of needle arrays.

3.1. Mechanism of needles formation

The formation of needle-shape stems from the microfluidic behavior of etchant solution confined in a small space [19,20]. As shown in the schematic drawing of Fig. 1d and SEM image of

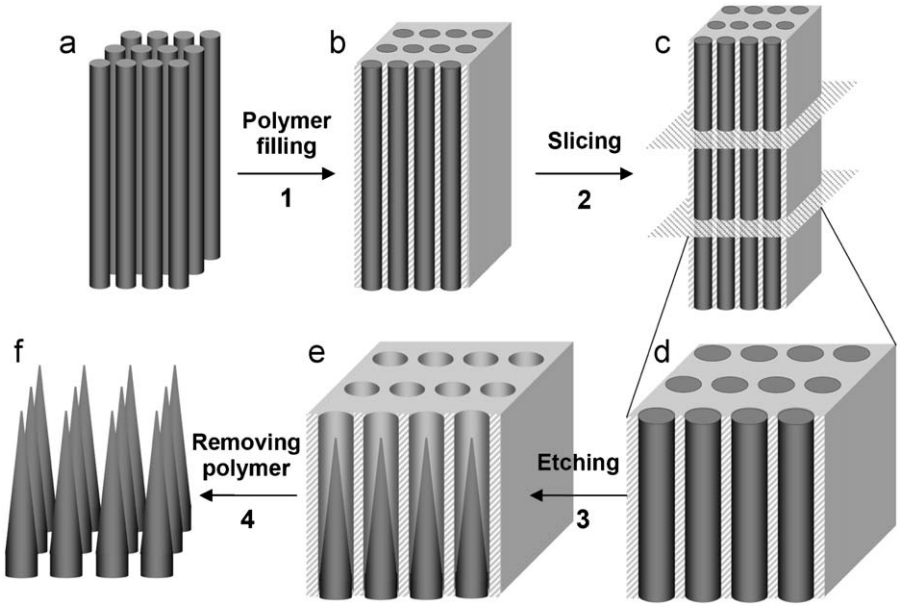

Fig. 1. Schematic illustration of the modularized processes for fabrication of silica needle arrays. The spacing of the needles and regions are exaggerated for clarity.

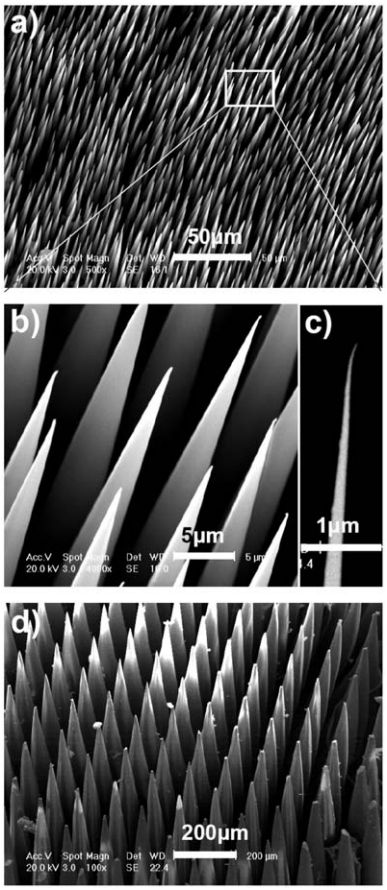

Fig. 2. SEM images (collected with a 70° tilt angle) of SNAs fabricated through a tube arrays fabrication and etching (TAFE) method: (a) needle array obtained from fibers of about 8 μm in diameter; (b) an enlarged observation on (a); (c) the details of a nanosized tip and (d) needle array obtained from fibers of about 125 μm in diameter.

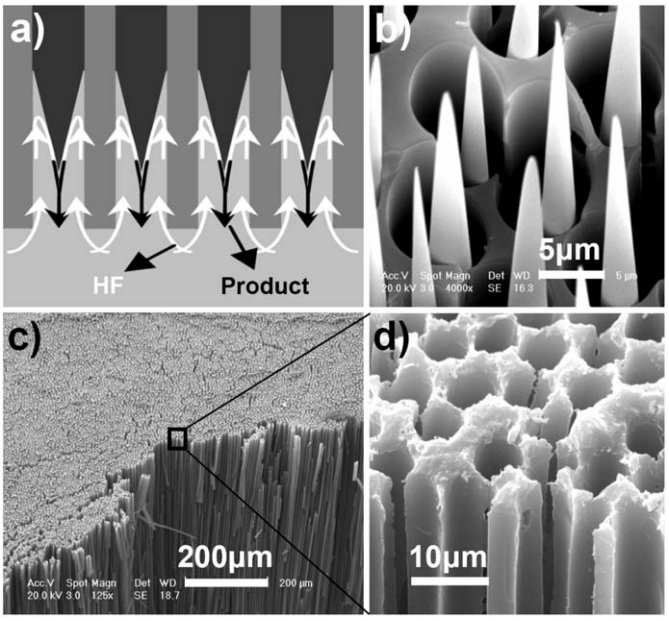

Fig. 3. Mechanism of tube-array-fabrication and etching (TAFE): (a) schematic explanation of the formation of needles confined in tube arrays; (b) SEM image of silica needles formed in the rosin tubes (ultrasonic treatment for about 1 min after HF etching, collected with a 70° tilt angle); (c) and (d) SEM of PMMA microtube arrays and their larger area view (collected with a 45° tilt angle).

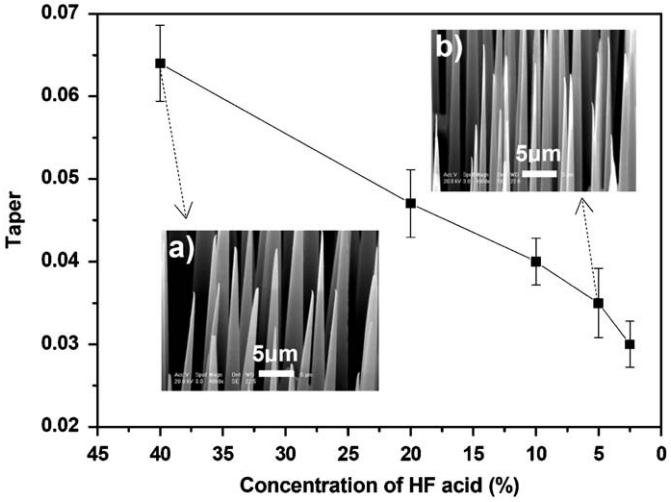

Fig. 4. Experimental results of the relationship between the taper and the etchant concentration for SNAs of about 8 μm in diameter. The SEM images of (a) and (b) show the typical results (collected with a 45° tilt angle).

Fig. 3b, the polymers (rosin or PMMA) constructed a tube arrays frame that works with silica fibers embedded in them. When they were immersed into the HF solution for etching, the silica is etched out but the rigid polymer frameworks retain their shape because of both their water and HF acid resistance. As a result, these nano/micro-tube arrays changed the fluid physics dramatically, which was schematically shown in Fig. 3a. At the initial stage, the etching rate of the outer regions was slightly faster than the center due to its larger HF volume supply and resulted in a conical shape [20]. As soon as the preliminary taper was formed, convection starts to deliver HF to the upper region of the cone and carry the dissolvent product out. The flow drives a preferential etching of the fiber edges, providing positive feedback that further reinforces the flow, which keep the cone shape during further etching. Indeed, the flow of liquid in a tube is quite complex during the etching. Understanding their detailed mechanisms was out of our motivation for the present work. A more professional explanation can be found in chemical fluid dynamics [21].

3.2. Needle size and taper tuning

The present method can be applied to fabricate SNAs of different diameters across ranges from tens of nanometers to hundreds of micrometers. As shown in Fig. 2, uniform needle arrays were acquired using silica fibers of various diameters as templates. The order of the needles is determined by the order of the silica fiber arrays. For example, ordered needle arrays were obtained by usage of mono-dispersed fibers as stacking units (Fig. 2d). Note that the bright parts in image of Fig. 2d were induced by a charging effect during the SEM observation, because the sidewalls of the structures cannot be covered with a connected conducting gold layer even after five times of gold sputtering.

The taper of a needle, defined as the ratio of fiber diameter to the needle height, is studied carefully. Generally, sharper tips were observed for needles created from thinner fibers. A taper of about 0.064 was found for needles created from fibers of about 8 μm in diameter. In contrast, a value of about 0.22 was observed for fibers of about 125 μm in diameter. For fibers of the same diameter of about 8 μm in diameter, we found that tapers of about 0.064, 0.047, 0.040, 0.035 and 0.030 corresponded to the HF solution of 40%, 20%, 10%, 5% and 2.5%, respectively, as shown in Fig. 4. But no apparent

changes in taper were found when the etching times varied from 30 min to 2 h. These results demonstrate that the tapers can be fine tuned by the concentrations of HF etchant. The character slightly dependent on etching time favors the needle arrays to be easily reproduced with high precision.

3.3. Orientation tuning

One of the unique advantages of the TAFE method is that it can precisely and arbitrarily tunes the orientations of the resulted needle arrays. As indicated in Fig. 5a, the needle arrays obliquity θ is adjusted by changing the cutting direction angle δ during the cutting process, where θ is defined as the angle between the needles and the cross of the needle arrays and δ is defined as the angle between the plane of the circular saw and the direction perpendicular to the fiber axis. Fig. 5b showed the resulted SNAs with obliquity θ of 45° (cutting direction angle δ=45°), and the needle arrays with obliquity θ of 90° (cutting direction angle δ=0°) were also given for comparison. The tilted needles were well aligned with tips directing to the designed direction. The taper of etch needle was almost the same for samples with different obliquity θ, which indicated the same etching process and mechanism. The resulted needle arrays may show some anisotropic properties for various applications, optics and mechanics, for example.

3.4. Creating super-hydrophobic surface with SNAs

The resulted micro-needle arrays provide an excellent template for generating microstructured surface with unique morphology, which may acquire many applications combined with various functional materials [22]. As an example for demonstration, we show that a super-hydrophobic surface can be created by covering the SNAs with a layer of PDMS. The coating was applied by dipping PDMS (Dow Corning Corporation, Sylgard 184) prepolymer mixture on their surface and let it flow freely. Then they were kept in oven at 120 °C for 30 min to make the PDMS fully cured. Fig. 6 shows the photographs of water (5 μL in volume) on flat and SNAs surfaces treated with PDMS. Because the drop was readily rolling down from the surface of PDMS treated SNAs, the stainless steel tip had to be left in contact with the drop during the measurement. The PDMS treated SNAs showed obvious

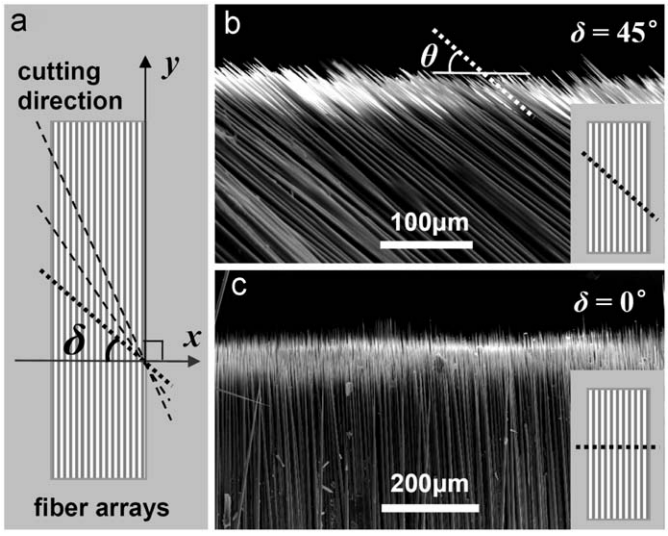

Fig. 5. (a) Schematic map of the cutting direction to tune the orientation of the fibers array; (b) and (c) show the SEM images of the resulted needle arrays with obliquity θ of 45°and 0°, respectively.

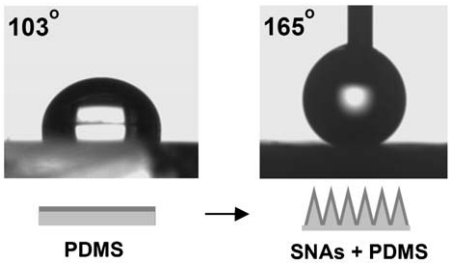

Fig. 6. Photographs of water on flat (left) and microstructured (right) surfaces treated with PDMS. Their contract angles are 103° and 165°, respectively.

super hydrophobic property with a contact angle of about 165°, in sharp contrast with the value of 103° for flat PDMS membrane. Actually, such a dewetting behavior on a rough surface had already been described by the well established models of Cassie [23]. It is assumed that the liquid forms a line of contact on the rough surface with air trapped below the line, and the effective contact angle θ^* can be formulated as

$$\cos\theta^* = \Phi(\cos\theta + 1) \quad (1)$$

where θ is the intrinsic contact angle measured on the flat surface, and Φ is the area fraction of the liquid–solid contact to the projected surface area.

The calculated Φ is 0.044 according to the above formula for contact angle of about 165°. Such a small Φ stems from the unique morphology of needle arrays. The diameter of the tips is about tens of nanometers with tip spacing of about 8 μm, and the large spacing/diameter ratio enables a tiny ratio of the liquid–solid contact area. Therefore, a super-hydrophobic surface can be generated as long as the ratio of the liquid–solid contact area to the overall projected area remains small enough [24].

4. Summary

In summary, we have presented a rapid and inexpensive strategy to fabricate sharp silica needle arrays with tunable tip orientations based on processes of polymer infiltration, cutting, chemical etching and polymer removal. Due to the massive and simplicity in fabrication, we believe that this method might promote various applications of such a unique morphology. For example, they show super hydrophobic property after being treated with PDMS. Furthermore, they can be used as templates to prepare other functional structures, or be covered with other functional materials and find applications in optic, energy harvesting, sensors, etc.

Acknowledgments

This work is supported by the State Key Program for Basic Research of China (no. 2007CB613202), National Natural Science Foundation of China (no. 50632030 and 60808025) and Ph.D. Programs Foundation of Ministry of Education of China (no. 20070284048).

References

[1] Z. Zhang, H. Yuan, J. Zhou, D. Liu, S. Luo, Y. Miao, Y. Gao, J. Wang, L. Liu, L. Song, Y. Xiang, X. Zhao, W. Zhou, S. Xie, J. Phys. Chem. B 110 (2006) 8566–8569.
[2] H.Z. Zhang, R.M. Wang, Y.W. Zhu, J. Appl. Phys. 96 (2004) 624–628.
[3] Y.W. Zhu, H.Z. Zhang, X.C. Sun, S.Q. Feng, J. Xu, Q. Zhao, B. Xiang, R.M. Wang, D.P. Yu, Appl. Phys. Lett. 83 (2003) 144–146.
[4] Q. Zhao, J. Xu, X.Y. Xu, Z. Wang, D.P. Yu, Appl. Phys. Lett. 85 (2004) 5331–5333.

[5] Y.F. Huang, S. Chattopadhyay, Y.J. Jen, C.Y. Peng, T.A. Liu, Y.K. Hsu, C.L. Pan, H.C. Lo, C.H. Hsu, Y.H. Chang, C.S. Lee, K.H. Chen, L.C. Chen, Nature Nanotech. 2 (2007) 770–774.
[6] M. Shen, J.E. Carey, C.H. Crouch, M. Kandyla, H.A. Stone, E. Mazur, Nano Lett. 8 (2008) 2087–2091.
[7] C.L. Chang, Y.F. Wang, Y. Kanamori, J.J. Shih, Y. Kawai, C.K. Lee, K.C. Wu, M. Esashi, J. Micromech. Microeng. 15 (2005) 580–585.
[8] J. Zhu, Z.F. Yu, G.F. Burkhard, C.M. Hsu, S.T. Connor, Y.Q. Xu, Q. Wang, M. McGehee, S.H. Fan, Y. Cui, Nano Lett. 9 (2009) 279–282.
[9] Y.Z. Huang, D.J.H. Cockayne, J. Ana-Vanessa, R.P. Cowburn, S.G. Wang, R.C.C. Ward, Nanotechnology 19 (2008) 015303.
[10] S. Jung, J. Yoo, Y. Kim, K. Kim, S.K. Dhungel, J. Yi, Mater. Sci. Eng. C 26 (2006) 813–817.
[11] M.R. Prausnitz, Adv. Drug Deliv. Rev. 56 (2004) 581–587.
[12] S. Henry, D.V. McAllister, M.G. Allen, M.R. Prausnitz, J. Pharm. Sci. 87 (1998) 922–925.
[13] C.H. Hsu, H.C. Lo, C.F. Chen, C.T. Wu, J.S. Hwang, D. Das, J. Tsai, L.C. Chen, K.H. Chen, Nano Lett. 4 (2004) 471–475.
[14] S.C. Shi, C.F. Chen, S. Chattopadhyay, Z.H. Lan, K.H. Chen, L.C. Chen, Adv. Funct. Mater. 15 (2005) 781–786.
[15] X.F. Wu, H. Bai, G.W. Lu, G.Q. Shi, Chem. Commun. (2006) 1655–1657.
[16] B. D'Urso, J.T. Simpson, M. Kalyanaraman, J. Micromech. Microeng. 17 (2007) 717–721.
[17] Z.Y. Ma, L.Y. Ma, M. Su, Adv. Mater. 20 (2008) 3734–3738.
[18] Z.Y. Ma, Y. Hong, L.Y. Ma, Y.L. Ni, S.L. Zou, M. Su, Langmuir 25 (2009) 643–647.
[19] P. Lambelet, A. Sayah, M. Pfeffer, C. Philipona, F. Marquis-Weible, Appl. Opt. 37 (1998) 7289–7292.
[20] R. Stöckle, C. Fokas, V. Deckert, R. Zenobia, B. Sick, B. Hecht, U.P. Wild, Appl. Phys. Lett. 75 (1999) 160–162.
[21] T.M. Squires, S.R. Quake, Rev. Mod. Phys. 77 (2005) 977–1026.
[22] L.S. Wan, Z.M. liu, Z.K. Xu, Soft Matter 5 (2009) 1775–1785.
[23] A.B.D. Cassie, S. Baxter, Trans. Faraday Soc. 40 (1944) 546–551.
[24] Z. Yoshimitsu, A. Nakajima, T. Watanabe, K. Hashimoto, Langmuir 18 (2002) 5818–5822.